

Discovery of Mer Specific Tyrosine Kinase Inhibitors for the Treatment and Prevention of Thrombosis

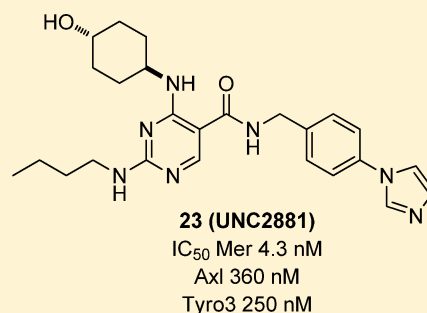
Weihe Zhang,^{†,‡,#} Andrew L. McIver,^{†,‡,#} Michael A. Stashko,^{†,‡} Deborah DeRyckere,[‡] Brian R. Branchford,[‡] Debra Hunter,[‡] Dmitri Kireev,^{†,‡} Michael J. Miley,[§] Jacqueline Norris-Drouin,^{†,‡} Wendy M. Stewart,^{†,‡} Minjung Lee,[‡] Susan Sather,[‡] Yingqiu Zhou,[‡] Jorge A. Di Paola,[‡] Mischa Machius,[§] William P. Janzen,^{†,‡} H. Shelton Earp,^{‡,§} Douglas K. Graham,[‡] Stephen V. Frye,^{†,‡,||} and Xiaodong Wang^{*,†,‡}

[†]Center for Integrative Chemical Biology and Drug Discovery [‡]Division of Chemical Biology and Medicinal Chemistry, Eshelman School of Pharmacy [§]Department of Pharmacology ^{||}Lineberger Comprehensive Cancer Center, Department of Medicine, School of Medicine, University of North Carolina at Chapel Hill, Chapel Hill, North Carolina 27599, United States

[‡]Department of Pediatrics, School of Medicine, University of Colorado Denver, Anschutz Medical Campus, Aurora, Colorado 80045, United States

S Supporting Information

ABSTRACT: The role of Mer kinase in regulating the second phase of platelet activation generates an opportunity to use Mer inhibitors for preventing thrombosis with diminished likelihood for bleeding as compared to current therapies. Toward this end, we have discovered a novel, Mer kinase specific substituted-pyrimidine scaffold using a structure-based drug design and a pseudo ring replacement strategy. The cocrystal structure of Mer with two compounds (7 and 22) possessing distinct activity have been determined. Subsequent SAR studies identified compound **23** (UNC2881) as a lead compound for in vivo evaluation. When applied to live cells, **23** inhibits steady-state Mer kinase phosphorylation with an IC₅₀ value of 22 nM. Treatment with **23** is also sufficient to block EGF-mediated stimulation of a chimeric receptor containing the intracellular domain of Mer fused to the extracellular domain of EGFR. In addition, **23** potently inhibits collagen-induced platelet aggregation, suggesting that this class of inhibitors may have utility for prevention and/or treatment of pathologic thrombosis.



INTRODUCTION

Platelets are small cells derived from precursor megakaryocytes. The physiologic procoagulant activity of platelets helps prevent excessive bleeding, while increased platelet activation and overactive coagulation can lead to pathologic thrombus formation which may result in stroke or heart attack. Antiplatelet compounds are therefore an important family of drugs for cardiovascular diseases and for certain surgical procedures where a risk of stroke or thrombosis is prevalent. However, current antiplatelet therapies are often complicated by significant bleeding and other side effects. For example, aspirin, an antiplatelet drug that functions through inhibiting the production of thromboxane, has a baseline major bleeding risk (gastrointestinal or intracranial) of 1–4%¹ and is associated with other toxicities including gastric side effects. The addition of clopidogrel (Plavix), another widely used antiplatelet drug, as a combination therapy further increases bleeding risk by 1%.² Moreover, not all patients respond to aspirin and clopidogrel: the nonresponse rates are 5.5–60% in patients treated with aspirin³ and 4–30% in those treated with clopidogrel⁴ based on meta-analyses. Consequently, there is still a significant need to develop novel therapies for treatment of thrombosis, especially

ones that do not increase the risk for bleeding and other side effects associated with current antithrombotic agents.

Mer is a member of the TAM (Tyro3, Axl and Mer) receptor tyrosine kinase (RTK) subfamily with growth-arrest-specific-6 (Gas6) as one of the endogenous ligands.⁵ Elevated Mer activation has been strongly associated with the oncogenesis of a number of human cancers.⁶ Recently, Mer has also been shown to play important roles in regulating macrophage activity and platelet aggregation.⁷ Mer knockout mice have decreased platelet aggregation while maintaining normal bleeding times and coagulation parameters. Consequently, these mice are protected from thrombosis without increased spontaneous bleeding.^{7a,8} These observations indicate that small molecule Mer kinase inhibitors have potential as new antiplatelet drugs with decreased bleeding complications, a profile that confers a major advantage over currently available antiplatelet therapies.

In our efforts to develop novel therapeutic agents for cancer treatment, we have discovered several potent small molecule Mer inhibitors. However, the first generation of these molecules possess either low selectivity for Mer relative to other TAM

Received: September 9, 2013

family members (**1** (UNC569))⁹ or low solubility and poor pharmacokinetic (PK) properties, such that they are not suitable for in vivo study (UNC1062).¹⁰ While efforts to optimize these molecules to yield a Mer selective, in vivo active pyrazolopyrimidine are ongoing, here we report the discovery of a new substituted-pyrimidine scaffold with significantly improved selectivity to further validate Mer as a potential target for thrombosis prevention.

In the cocrystal structure of Mer in complex with compound **1** (Figure 1A),⁹ the inhibitor is fully confined to the relatively

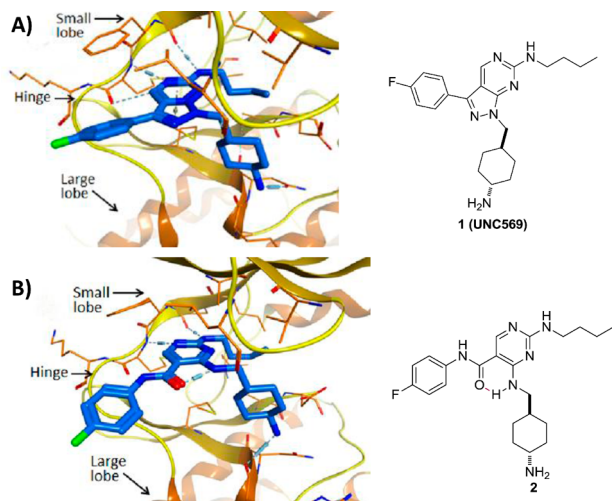


Figure 1. Structure-based design of a scaffold that features pseudo ring formation through an intramolecular hydrogen bond. (A) X-ray structure of **1** complexed with Mer protein (kinase domain) (PDB ID code 3TCP). (B) Docking model (based on X-ray structure PDB ID code 3TCP) of the designed molecule **2**.

small adenine pocket, forming three hydrogen bonds: two with the hinge region of Mer using one nitrogen of the pyrimidine ring (with residue Met674) and the NH from the butyl amino side chain (with residue Pro672) and another one with the carbonyl of Arg727 via the methylcyclohexylamino group. Because the pyrazole ring does not appear to interact with the Mer active site directly, its major role may be to rigidify the molecule. Therefore, replacement of the pyrazole ring with a pseudo ring¹¹ constrained by an intramolecular hydrogen bond while maintaining functionality to create the three hydrogen bonds observed with **1** may mimic the binding conformation in

Figure 1A and retain the potency observed with compound **1**. One such design is shown in Figure 1B, where the intramolecular hydrogen bond in **2** will be formed between the carbonyl oxygen of the amide group and the hydrogen on the adjacent amino side chain. The other substituents are not modified and will likely occupy the same regions as in **1**. However, because the pseudo ring is less rigid and larger in size than the pyrazole ring, this new scaffold may have a distinct kinase specificity profile or pharmacokinetic (PK) properties due to subtle conformational and physical property changes. Furthermore, the synthesis of **2** is straightforward making efficient structure–activity relationship (SAR) studies feasible.

CHEMISTRY

The syntheses of pyrimidine analogues are shown in Scheme 1. An amide coupling reaction is used to introduce the R¹ group while an S_NAr reaction is used to introduce the R² and R³ groups. Path A is designed for SAR exploration of the R² and R³ positions, while path B is designed for diversifying the R¹ position.

RESULTS AND DISCUSSION

To test our pseudo ring replacement hypothesis, a small set of compounds were synthesized using the route depicted in Scheme 1 (compounds **3** and **5** started with 2,4-dichloropyrimidin-5-amine and 4-fluorobenzoyl chloride) (Table 1). Inhibition of Mer kinase activity by these compounds was tested using a microfluidic capillary electrophoresis (MCE) assay.¹² Indeed, compound **2** was very potent against Mer while its close analogue **3** exhibited only weak activity. The only structural difference between **2** and **3** was the regiochemistry of the key hydrogen bond, enabling amide functionality. The reverse amide bond in **3** is unable to form the pseudo ring forming intramolecular hydrogen bond with the hydrogen on the amino side chain at the R² position resulting in greatly diminished Mer activity. Comparison of the activity of **4** and **5** further confirmed the important role of the intramolecular hydrogen bond and validated our design of the pseudo ring replacement. To monitor selectivity within the TAM family, the ability of these analogues to inhibit Axl and Tyro3 was also tested, and they were significantly more active against Mer than Axl and Tyro3 (Table 1). In addition, the *trans*-4-aminocyclohexylmethylamino group at the R² position in **2** can be replaced by a *trans*-4-hydroxycyclohexylamino group in **4** and the activity against Mer is retained. In our previous studies, the

Scheme 1. Synthetic Routes for Pyrimidine Analogues

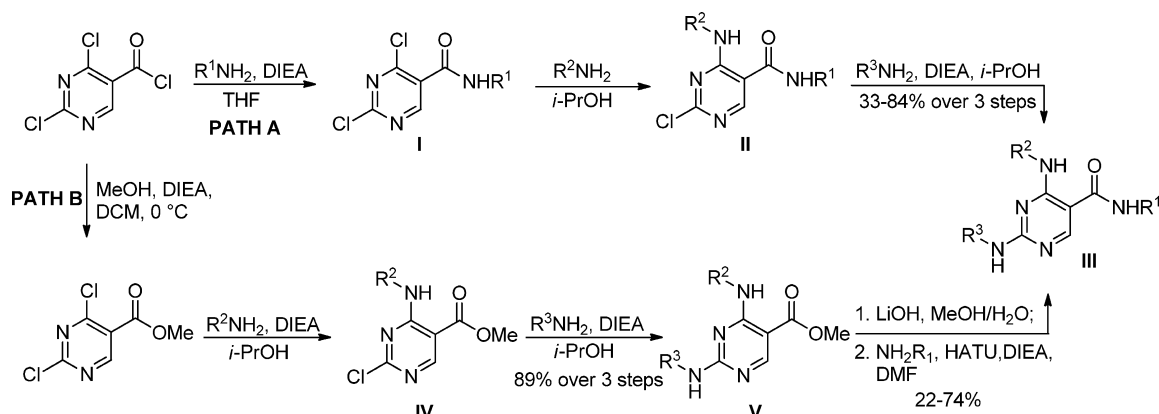
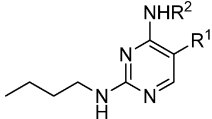
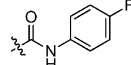
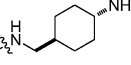
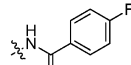
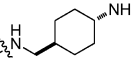
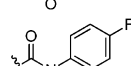
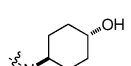
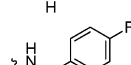
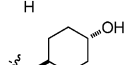


Table 1. Key SAR Observations

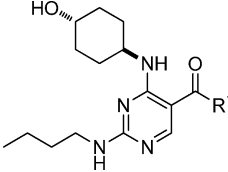


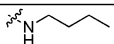
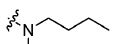
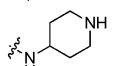
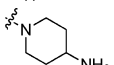
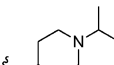
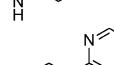
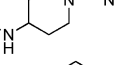
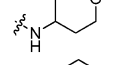
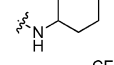
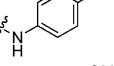
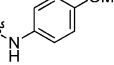
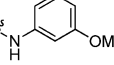
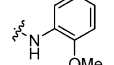
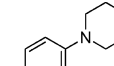
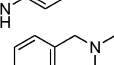
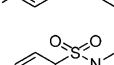
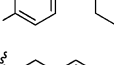
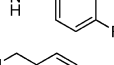
Compound	R ¹	NHR ²	IC ₅₀ (μM) ^a		
			Mer	Axl	Tyro3
2			0.040	2.0	0.90
3			12.6	>30	>30
4			0.023	1.7	2.2
5			>30	>30	>30

^aValues are the mean of two or more independent assays.

primary amino group at the R² position could result in undesired hERG activity.^{10a} Therefore, the *trans*-4-hydroxycyclohexylamino group was used at the R² position for further SAR exploration at the R¹ site.

Next, a focused library of compounds with different R¹ groups was synthesized while keeping R³ fixed as a butylamino group (Table 2). Interestingly, the amide nitrogen at the R¹ site could not be further substituted. Even simple methylation of the amide bond almost abolished the Mer activity (6 vs 7 and 8 vs 9). This may be due to weaker binding of the ligand to the hinge motif (residues 672–677). Not only does amide methylation of the ligand preclude a hydrogen bond to the Met674-backbone carbonyl, it also contributes to a less favorable orientation of the aminopyrimidine group with respect to Pro672 and Met674. Because 8 was more active than the open chain analogue 6, our focus was initially on further modification of 8. However, the addition of extra groups such as ⁱPr (10) and pyrimidine (11) to the nitrogen of the piperidine ring did not boost the activity. Exchange of the piperidine nitrogen with oxygen (12) or carbon (13) also did not significantly affect the activity. Interestingly, when the piperidine ring was replaced with an aromatic ring, the activity of the analogues was modulated by the substituents on the aromatic ring: an electron-withdrawing group such as CF₃ on the aromatic ring yielded a much weaker Mer inhibitor (14) compared to 8, while an electron-donating group like MeO on the aromatic ring produced an analogue with similar activity (15). Inhibition of Mer was not sensitive to the substitution pattern on the aromatic ring (15–17). In addition, larger groups such as morpholine (18), morpholinomethyl (19), and morpholinosulfonyl (which was the R¹ group of UNC1062^{10a}) (20) could be tolerated on the aromatic ring. This is consistent with the prediction that the R¹ group interacting with the solvent front based on the docking model. Furthermore, a methylene group could be inserted between the amide bond and the aromatic ring without a change in activity (4 vs 21, Table 1). However, the activity of the analogues was increased by introducing a larger group on the aromatic ring as in 22 and 23 (UNC2881). In general, these analogues are significantly

Table 2. Preliminary SAR at the R¹ Position


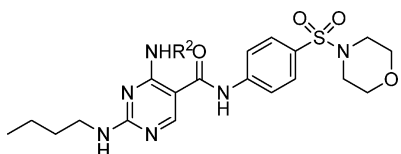
Compound	R ¹	IC ₅₀ (μM) ^a		
		Mer	Axl	Tyro3
6		0.067	3.0	6.7
7		5.9	>30	>30
8		0.0090	0.48	0.53
9		2.5	>30	>30
10		0.0084	0.43	0.19
11		0.0041	0.56	0.48
12		0.013	0.58	0.54
13		0.0080	0.37	0.37
14		0.23	16.6	17.9
15		0.015	0.88	0.66
16		0.029	1.7	0.83
17		0.039	3.8	1.5
18		0.014	0.57	0.45
19		0.0067	0.37	0.24
20		0.0063	0.53	0.70
21		0.014	0.79	0.57
22		0.0052	0.26	0.28
23		0.0043	0.36	0.25

^aValues are the mean of two or more independent assays.

more Mer-selective than **2**, especially compound **23** (84-fold over Axl and 58-fold over Tyro3).

In addition, we explored SAR at the R² site while keeping R¹ fixed as morpholinosulfonylphenyl carboxamide and R³ fixed as butylamino group. A few examples are included in Table 3.

Table 3. SAR Study of R²



Compound	NHR ²	IC ₅₀ (μM) ^a		
		Mer	Axl	Tyro3
24		0.0021	0.40	0.40
25		0.59	>30	>30
26		0.037	4.7	0.62
27		0.14	14.0	1.6
28		0.062	10.7	2.0
29		1.0	>30	19.5
30		0.11	12.6	2.0
31		0.62	21	4.1
32		0.17	>30	>30
33		9.9	>30	>30

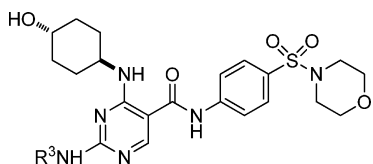
^aValues are the mean of two or more independent assays.

When introducing the *trans*-4-aminocyclohexylamino group at the R² site, the corresponding analogue **24** had activity similar to **20** (Table 2). However, removal of the polar group NH₂ on the cyclohexyl ring (**25**) reduced the activity dramatically (over 280-fold). This is consistent with the SAR observed with analogues of **1**: a hydrogen bond between a polar substituent at the R² position with the carbonyl of Arg727 of the Mer protein is important.⁹ Compared to **25**, secondary amines such as 4-piperidinylmethylamino (**26**), (*R*)-3-piperidinylmethylamino (**27**), and 4-piperidinylamino (**28**) at the R² position increased the activity compared to **25** but were less suitable than the primary amine group. Interestingly, introduction of an (*S*)-3-pyrrolodinyllamino group in (**30**) led to a 9-fold higher activity compared to the (*R*)-3-pyrrolodinyllamino substitution (**29**). The structural analysis suggests that this 9-fold activity gain is most likely due to an optimal interaction of the pyrrolidine nitrogen in **30** with the backbone carbonyl of Leu593, while the same nitrogen in **29** would not be able to optimally approach Leu593. A 4 substituted-pyridine ring at the R² position resulted in a much less active analogue **31** than the corresponding 4 substituted-piperidine ring (**26**). Replacement of the 4-piperidinylamino group (**28**) with a 4-pyranylamino

group (**32**) decreased the activity slightly. However, a morpholine at the R² position (**33**) almost abolished the Mer activity due to the absence of the pseudo ring forming intramolecular hydrogen bond. In general, these analogues have good selectivity for Mer over Axl and Tyro3.

The SAR at the R³ position was further explored while fixing R¹ as a morpholinosulfonylphenyl carboxamide group and R² as a *trans*-4-hydroxycyclohexylamino group (Table 4). Absence of

Table 4. SAR Study of R³



Compound	NHR ³	IC ₅₀ (μM) ^a		
		Mer	Axl	Tyro3
34		2.4	16.6	>30
35		0.15	1.2	>30
36		0.037	0.78	16.2
37		0.011	0.61	1.2
38		0.027	1.1	21.9
39		0.0073	0.30	0.94
40		0.086	5.7	5.1
41		0.059	4.3	6.7
42		0.024	1.9	1.7
43		0.047	9.0	4.3
44		0.18	7.4	2.3
45		0.12	>30	>30
46		>30	>30	>30
47		>30	>30	>30

^aValues are the mean of two or more independent assays.

substitution on the amino group at the R³ position resulted in only a weak Mer inhibitor (**34**), and even a methyl group at this position significantly increased the activity (16-fold) (**35** vs **34**). Analogues were progressively more active with addition of longer alkyl side chains (**36** and **37**) until the chain reached 4-carbons in length (**20** (Table 2); the activity began to decrease when the chain was 5-carbons (**38**) or longer. A cyclopropyl group (**39**) was tolerated at the end of the propyl side chain, while a polar group, such as trifluoromethyl (**40**) or a hydroxyl group (**41**), was less tolerated. A branched alkyl side chain did not significantly affect activity (**42** vs **36**). However, cyclohexyl (**43**), 4-tetrahydropyranyl (**44**), or 4-fluorobenzyl (**45**) at this

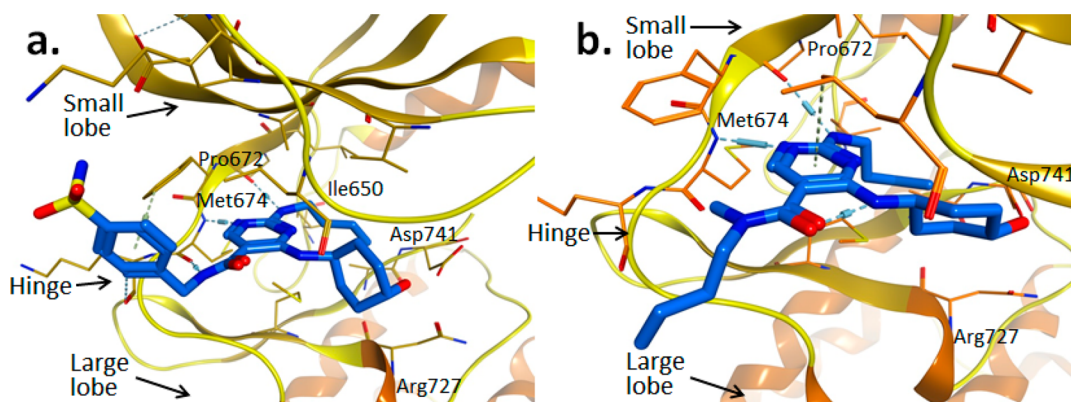


Figure 2. X-ray structures of compounds **22** (PDB ID code 4MHA) (a) and **7** (PDB code 4MH7) (b) in complex with the Mer kinase domain.

Table 5. PK Profile of 23

route ^a	<i>T</i> _{1/2} (h)	<i>T</i> _{max} (h)	<i>C</i> _{max} (ng/mL)	AUC _{last} (h·ng/mL)	Cl _{obs} (mL/min/kg)	V _{ss} (L/kg)	%F
IV	0.80		2609	527	94.5	1.65	
PO		0.30	90.0	71.7			14

^aA dose of 3 mg/kg for both routes.

position decreased Mer activity. Furthermore, when the amino group at this position was fully substituted, as in **46** and **47**, Mer activity was completely eliminated. This result is consistent with our design hypothesis where the nitrogen of the amino group of R³ forms a hydrogen bond with residue Pro672 at Mer protein hinge area. Again, these analogues are Mer-selective as compared to Axl and Tyro3.

To characterize the binding interactions of the reported pyrimidine inhibitors with Mer and provide a structural basis for future directions in chemical optimization, cocrystal structures of Mer in complex with compounds **7** and **22** were obtained. The structures in Figure 2 demonstrate a binding mode in which the pyrimidine ring inserts into the adenine binding site and mimics interactions of the adenine with the backbone atoms of the hinge (residues Pro672 and Met674). Similar to the previously published Mer-1 complex,⁹ the butyl amino side chain (R³ substituent) is folded into the relatively small adenine site instead of protruding into the lipophilic back-pocket. However, unlike the previously published structure, the hydroxyl group of the R² substituent forms a hydrogen bond with the side chain of Asp741 instead of the nearby Arg727 (as does the R² amino group of **1**). It is noteworthy that one of the gate-forming residues, Ile650, is not conserved among other members of the TAM subfamily, Axl and Tyro3, which feature methionine and alanine in this position, respectively. This variability is quite likely the reason for the significant intrafamily selectivity observed. It is remarkable that despite sharing identical core motifs, compounds **7** and **22** display very different IC₅₀ values of 5.9 and 0.0052 μM, respectively. The most likely explanation for this significant difference is that the methyl group substituted on the amide of compound **7** precludes a hydrogen bond to the Met674 backbone carbonyl (present in the compound **22**:Mer complex) and may also prevent the aminopyrimidine group from binding to Pro672 and Met674 in the most favorable orientation. Consistent with the SAR discussed above, the R¹ substituent interacts mostly with the solvent and does not significantly impact the activity. Consequently, it can be utilized for tuning solubility and other physical or PK properties.

On the basis of its solubility, inhibitory activity against Mer, and remarkable intrafamily selectivity, **23** was chosen as a lead compound in this series. The in vivo PK properties of **23** were assessed in mice via both intravenous (IV) and oral (PO) administration (Table 5). **23** had high systemic clearance (94.5 mL/min/kg) and 14% oral bioavailability. The terminal half-life was 0.80 h. The volume of distribution was 2-fold greater than the normal volume of total body water (0.70 L/kg). Although the PK properties of **23** are not yet ideal and need to be further improved to enable chronic in vivo studies, this compound is sufficient for in vitro or short-term in vivo studies.

The inhibitory activity mediated by **23** against a panel of 30 kinases was also determined at a concentration 100-fold above its Mer IC₅₀ (Figure 3) (details in Supporting Information). This experiment provides a broad survey of kinase families emphasizing tyrosine kinases along with a selection of serine/threonine kinases. Six kinases were inhibited by greater than 50% in the presence of 430 nM **23**, while none of the serine/threonine kinases were appreciably inhibited.

When **23** was tested in cell-based assays, it mediated inhibition of Mer phosphorylation in 697 B-ALL cells with an IC₅₀ value of 22 nM (Figure 4). In addition to this effect on steady-state levels of phosphorylated Mer, **23** efficiently inhibited ligand-dependent phosphorylation of a chimeric protein consisting of the extracellular domain from the epidermal growth factor (EGF) receptor and the intracellular domain of Mer (Figure 5). Moreover, treatment with **23** inhibited platelet aggregation by greater than 25% in human platelet-rich plasma in response to stimulation with fibrillar type I equine collagen (Figure 6). ATP release, which is a marker of platelet activation and degranulation, was decreased to a similar extent. These data are the first to demonstrate functional inhibition of platelet activity mediated by a Mer-selective small molecule tyrosine kinase inhibitor and suggest the utility of Mer inhibitors for this therapeutic application.

CONCLUSIONS

We have successfully applied a pseudo ring replacement strategy to discover a potent substituted-pyrimidine series as new Mer kinase selective inhibitors. The cocrystal structures of

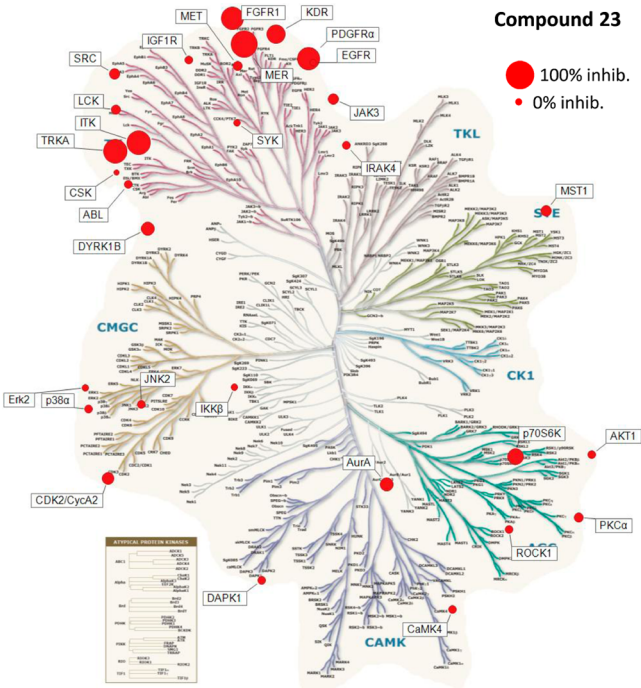


Figure 3. Kinase tree.

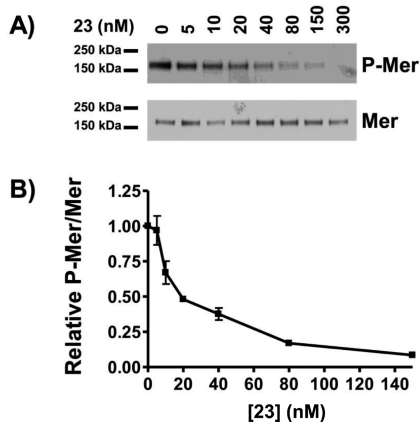


Figure 4. 23 inhibits endogenous Mer tyrosine kinase activation in acute lymphoblastic leukemia cells. 697 B-ALL cells were treated with the indicated concentrations of 23 for 1 h. Pervanadate was added to cultures for 3 min to stabilize the phosphorylated form of Mer. Mer was immunoprecipitated from cell lysates, and total Mer protein and Mer phosphoprotein were detected by immunoblot. (A) Representative Western blots. (B) Relative levels of phospho-Mer and Mer proteins were determined. Mean values \pm standard error derived from three independent experiments are shown. $IC_{50} = 21.9$ nM with a 95% confidence interval of 16.9–28.5 nM.

7 and 22 with Mer protein have been determined and their binding modes provide a rationale for the 1000-fold difference in their IC_{50} values. The lead compound 23 inhibited Mer kinase activity in cell-based assays and mediated functional inhibition of human platelet activation, suggesting the utility of Mer-selective small molecule inhibitors for treatment and/or prevention of pathologic thrombosis.

EXPERIMENTAL SECTION

Details on the synthesis of all compounds are given in the Supporting Information. The purity of all tested compounds was determined by LC/MS to be >95%.

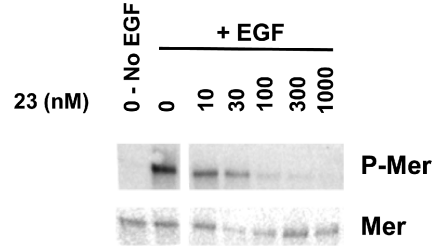


Figure 5. 23 inhibits ligand-stimulated activation of a chimeric EGFR-MerTK. 32D cells expressing a chimeric receptor consisting of the extracellular ligand-binding domain of the EGF receptor and the intracellular domain of Mer were treated with 23 or vehicle for 1 h prior to stimulation with 100 ng/mL EGF ligand for 15 min. Mer was immunoprecipitated from whole cell lysates and phospho-tyrosine containing and total Mer proteins were detected by Western blot. Results shown are representative of two independent experiments.

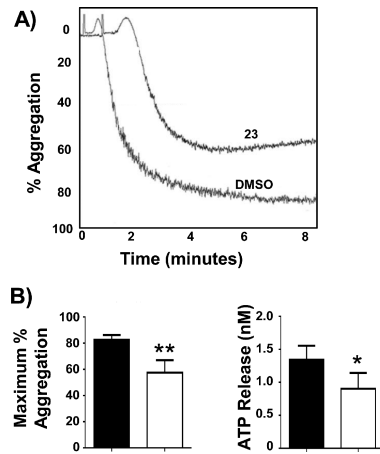


Figure 6. 23 inhibits collagen-stimulated platelet aggregation. Human platelet-rich plasma was normalized to a platelet count of 250000/ μ L with platelet-poor plasma obtained by differential centrifugation. Samples were treated with 3 μ M 23 or DMSO vehicle for 1 h at room temperature prior to stimulation with 1 μ g/mL type I equine fibrillar collagen and assessment of aggregation and ATP release using an aggregometer. (A) Representative aggregation from samples treated with 3 μ M 23 or DMSO. (B) Maximum percent aggregation and ATP release are shown for samples treated with 23 or DMSO vehicle. Mean values \pm SEM derived using plasma collected from five (ATP release) or seven (aggregation) different individuals are shown. Statistically significant results were determined using the student's paired t test (* $p = 0.05$ and ** $p = 0.01$ relative to vehicle control).

Microfluidic Capillary Electrophoresis (MCE) Assay.⁹ Activity assays were performed in a 384 well, polypropylene microplate in a final volume of 50 μ L of 50 mM Hepes, pH 7.4 containing 10 mM $MgCl_2$, 1.0 mM DTT, 0.01% Triton X-100, 0.1% bovine serum albumin (BSA), containing 1.0 μ M fluorescent substrate (Table 6) and ATP at the K_m for each enzyme (Table 6). All reactions were terminated by addition of 20 μ L of 70 mM EDTA. After a 180 min incubation, phosphorylated and unphosphorylated substrate peptides (Table 6) were separated in buffer supplemented with 1 \times CR-8 on a

Table 6. Assay Conditions for MCE Assays

kinase	peptide substrate	kinase (nM)	ATP (μ M)
Mer	5-FAM-EFPIYDFLPAKKK-CONH ₂	2.0	5.0
Axl	5-FAM-KKKKEEYFFF-CONH ₂	120	65
Tyro	5-FAM-EFPIYDFLPAKKK-CONH ₂	10	21

LabChip EZ Reader equipped with a 12-sipper chip. Data were analyzed using EZ Reader software.

Cell-Based Assays for Mer Kinase Inhibition. 697 B-ALL Cell Assay. 697 B-ALL cells were cultured in the presence of 23 or vehicle only for 1.0 h. Pervanadate solution was prepared fresh by combining 20 mM sodium orthovanadate in 0.9× PBS in a 1:1 ratio with 0.3% (w/w) hydrogen peroxide in PBS for 15–20 min at room temperature. Cultures were treated with 120 μ M pervanadate prior to collection for preparation of whole cell lysates, immunoprecipitation of Mer, and analysis by Western blot.

Then 697 B-ALL cells were treated with pervanadate for 3.0, 5.0, and 1.0 min, respectively. Cell lysates were prepared in 50 mM HEPES pH 7.5, 150 mM NaCl, 10 mM EDTA, 10% glycerol, and 1% Triton X-100, supplemented with protease inhibitors (Roche Molecular Biochemicals, no. 11836153001). Mer protein was immunoprecipitated with a monoclonal anti-Mer antibody (R&D Systems, no. MAB8912) and Protein G agarose beads (Invitrogen). Phospho-Mer was detected by Western blot using a polyclonal antiphospho-Mer antibody raised against a peptide derived from the triphosphorylated activation loop of Mer. Nitrocellulose membranes were stripped and total Mer protein was detected using a second anti-Mer antibody (Epitomics Inc., no. 1633-1). For 697 B-ALL cells, relative phosphorylated and total Mer protein levels were determined by densitometry using Image J software and IC₅₀ values were determined by nonlinear regression.

32D-EMC Cell Assay. 32D-EMC suspension cultures were treated with the indicated concentration of 23 or vehicle before stimulation with 100 ng/mL EGF (BD Biosciences no. 354010) for 15 min. Cells were centrifuged at 1000g for 5 min and washed with 1× PBS. Cell lysates were prepared in 20 mM HEPES (pH 7.5), 50 mM NaF, 500 mM NaCl, 5.0 mM EDTA, 10% glycerol, and 1% Triton X-100, supplemented with protease inhibitors (10 μ g/mL leupeptin, 10 μ g/mL phenylmethylsulfonyl fluoride, and 20 μ g/mL aprotinin) and phosphatase inhibitors (50 mM NaF and 1.0 mM sodium orthovanadate), and Mer protein was immunoprecipitated using a custom polyclonal rabbit anti-Mer antisera raised against a GST protein derived from the C-terminus of human Mer and Protein A agarose beads (Santa Cruz Biotechnology). Phosphotyrosine-containing proteins were detected by Western blot with a monoclonal HRP-conjugated antiphosphotyrosine antibody (Santa Cruz Biotechnology, no. sc-508). Antibodies were stripped from membranes and total Mer levels were determined using the custom polyclonal rabbit anti-Mer antibody raised against a peptide derived from the catalytic domain of Mer.

Platelet Aggregation Assay. Human whole blood (WB) was collected from healthy volunteers as permitted by an Institutional Review Board-approved protocol (COMIRB no. 09-0816). WB was drawn by venipuncture into 3.8% sodium citrate and centrifuged at 200g for 20 min at room temperature. Platelet-rich plasma (PRP) was separated, and the remaining solution was spun at 2400g for 10 min to create platelet-poor plasma (PPP). PRP and PPP were mixed in appropriate proportions to obtain a final concentration of 2.5×10^5 platelets/ μ L and then used within 3 h of the initial blood draw.

For platelet aggregation assays, plasma was incubated for 60 min at RT with either 3 μ M 23 or vehicle (20% DMSO in saline). Samples were analyzed using a light-transmission aggregometer (CHRONO-LOG Corporation, Havertown, PA) at 37 °C in the presence of Chrono-lume reagent (CHRONO-LOG) with magnetic stirring at 1200 rpm and addition of 1 μ g/mL equine type I fibrillar collagen (CHRONO-LOG) as an aggregation agonist. Optical density was determined as an indicator of aggregation. Emission of light by Chrono-lume, a luciferin-luciferase compound, occurs as a result of ATP binding and is determined relative to a 2 nM standard as a measure of the amount of ATP released from activated platelets. ATP release (nM) and the maximum percent aggregation were recorded 7 min after collagen addition.

■ ASSOCIATED CONTENT

● Supporting Information

Experimental details, characterization of all compounds, and selectivity profiling. This material is available free of charge via the Internet at <http://pubs.acs.org>.

Accession Codes

The atomic coordinates for the X-ray crystal structures of 7 and 22 have been deposited with the RCSB Protein Data Bank under the accession code 4MH7 and 4MHA.

■ AUTHOR INFORMATION

Corresponding Author

*Phone: 919-843-8456. E-mail: xiaodonw@unc.edu.

Author Contributions

*W.Z. and A.M. contributed equally.

Notes

The authors declare the following competing financial interest(s): DD, DK, WPJ, HSE, DG, SF, and XW hold equity of Meryx, Inc.

■ ACKNOWLEDGMENTS

This work was supported by the University Cancer Research Fund and Federal Funds from the National Cancer Institute, National Institute of Health, under contract no. HHSN261200800001E. The content of this publication does not necessarily reflect the views or policies of the Department of Health and Human Services, nor does mention of trade names, commercial products, or organizations imply endorsement by the U.S. Government.

■ REFERENCES

- (1) De Berardis, G.; Lucisano, G.; D'Ettorre, A.; et al. Association of aspirin use with major bleeding in patients with and without diabetes. *JAMA, J. Am. Med. Assoc.* **2012**, 307 (21), 2286–2294.
- (2) Diener, H.-C.; Bogousslavsky, J.; Brass, L. M.; Cimminiello, C.; Csiba, L.; Kaste, M.; Leys, D.; Matias-Guiu, J.; Rupprecht, H.-J. Aspirin and clopidogrel compared with clopidogrel alone after recent ischaemic stroke or transient ischaemic attack in high-risk patients (MATCH): randomised, double-blind, placebo-controlled trial. *Lancet* **2004**, 364 (9431), 331–337.
- (3) Sanderson, S.; Emery, J.; Baglin, T.; Kinmonth, A.-L. Narrative Review: Aspirin Resistance and Its Clinical Implications. *Ann. Intern. Med.* **2005**, 142 (5), 370–380.
- (4) Nguyen, T. A.; Diodati, J. G.; Pharand, C. Resistance to clopidogrel: a review of the evidence. *J. Am. Coll. Cardiol.* **2005**, 45 (8), 1157–1164.
- (5) Laurance, S.; Lemarie, C. A.; Blostein, M. D. Growth Arrest-Specific Gene 6 (gas6) and Vascular Hemostasis. *Adv. Nutr.* **2012**, 3 (2), 196–203.
- (6) Linger, R. M. A.; Keating, A. K.; Earp, H. S.; Graham, D. K., TAM Receptor Tyrosine Kinases: Biologic Functions, Signaling, and Potential Therapeutic Targeting in Human Cancer. In *Advances in Cancer Research*, Academic Press: New York, 2008; Vol. 100, pp 35–83.
- (7) (a) Chen, C. L.; Li, Q.; Darrow, A. L.; Wang, Y. P.; Derian, C. K.; Yang, J.; de Garavilla, L.; Andrade-Gordon, P.; Damiano, B. P. Mer receptor tyrosine kinase signaling participates in platelet function. *Arterioscl. Thromb. Vasc. Biol.* **2004**, 24 (6), 1118–1123. (b) Chen, J.; Carey, K.; Godowski, P. J. Identification of Gas6 as a ligand for Mer, a neural cell adhesion molecule related receptor tyrosine kinase implicated in cellular transformation. *Oncogene* **1997**, 14 (17), 2033–2039. (c) Sather, S.; Kenyon, K. D.; Lefkowitz, J. B.; Liang, X.; Varnum, B. C.; Henson, P. M.; Graham, D. K. A soluble form of the Mer receptor tyrosine kinase inhibits macrophage clearance of

apoptotic cells and platelet aggregation. *Blood* **2007**, *109* (3), 1026–1033.

(8) Angelillo-Scherrer, A.; Burnier, L.; Flores, N.; Savi, P.; DeMol, M.; Schaeffer, P.; Herbert, J. M.; Lemke, G.; Goff, S. P.; Matsushima, G. K.; Earp, H. S.; Vesin, C.; Hoylaerts, M. F.; Plaisance, S.; Collen, D.; Conway, E. M.; Wehrle-Haller, B.; Carmeliet, P. Role of Gas6 receptors in platelet signaling during thrombus stabilization and implications for antithrombotic therapy. *J. Clin. Invest.* **2005**, *115* (2), 237–246.

(9) Liu, J.; Yang, C.; Simpson, C.; DeRyckere, D.; Van, D. A.; Miley, M. J.; Kireev, D.; Norris-Drouin, J.; Sather, S.; Hunter, D.; Korboukh, V. K.; Patel, H. S.; Janzen, W. P.; Machius, M.; Johnson, G. L.; Earp, H. S.; Graham, D. K.; Frye, S. V.; Wang, X. Discovery of Small Molecule Mer Kinase Inhibitors for the Treatment of Pediatric Acute Lymphoblastic Leukemia. *ACS Med. Chem. Lett.* **2012**, *3*, 129–134.

(10) (a) Liu, J.; Zhang, W.; Stashko, M. A.; DeRyckere, D.; Cummings, C. T.; Hunter, D.; Yang, C.; Jayakody, C. N.; Cheng, N.; Simpson, C.; Norris-Drouin, J.; Sather, S.; Kireev, D.; Janzen, W. P.; Earp, H. S.; Graham, D. K.; Frye, S. V.; Wang, X. UNC1062, a new and potent Mer inhibitor. *Eur. J. Med. Chem.* **2013**, *65*, 83–93. (b) Schlegel, J.; Sambade, M. J.; Sather, S.; Moschos, S. J.; Tan, A. C.; Wings, A.; Deryckere, D.; Carson, C. C.; Trembath, D. G.; Tentler, J. J.; Eckhardt, S. G.; Kuan, P. F.; Hamilton, R. L.; Duncan, L. M.; Miller, C. R.; Nikolaishvili-Feinberg, N.; Midkiff, B. R.; Liu, J.; Zhang, W.; Yang, C.; Wang, X.; Frye, S. V.; Earp, H. S.; Shields, J. M.; Graham, D. K. MERTK receptor tyrosine kinase is a therapeutic target in melanoma. *J. Clin. Invest.* **2013**, *123* (5), 2257–2267.

(11) (a) Mathieu, S.; Gradl, S. N.; Ren, L.; Wen, Z.; Aliagas, I.; Gunzner-Toste, J.; Lee, W.; Pulk, R.; Zhao, G.; Alicke, B.; Boggs, J. W.; Buckmelter, A. J.; Choo, E. F.; Dinkel, V.; Gloor, S. L.; Gould, S. E.; Hansen, J. D.; Hastings, G.; Hatzivassiliou, G.; Laird, E. R.; Moreno, D.; Ran, Y.; Voegtli, W. C.; Wenglowsky, S.; Grina, J.; Rudolph, J. Potent and Selective Aminopyrimidine-Based B-Raf Inhibitors with Favorable Physicochemical and Pharmacokinetic Properties. *J. Med. Chem.* **2012**, *55* (6), 2869–2881. (b) Zhang, G.; Ren, P.; Gray, N. S.; Sim, T.; Liu, Y.; Wang, X.; Che, J.; Tian, S.-S.; Sandberg, M. L.; Spalding, T. A.; Romeo, R.; Iskandar, M.; Chow, D.; Martin Seidel, H.; Karanewsky, D. S.; He, Y. Discovery of pyrimidine benzimidazoles as Lck inhibitors: Part I. *Bioorg. Med. Chem. Lett.* **2008**, *18* (20), 5618–5621. (c) Furet, P.; Caravatti, G.; Guagnano, V.; Lang, M.; Meyer, T.; Schoepfer, J. Entry into a new class of protein kinase inhibitors by pseudo ring design. *Bioorg. Med. Chem. Lett.* **2008**, *18* (3), 897–900.

(12) (a) Pommereau, A.; Pap, E.; Kannt, A. Two simple and generic antibody-independent kinase assays: comparison of a bioluminescent and a microfluidic assay format. *J. Biomol. Screening* **2004**, *9* (5), 409–416. (b) Dunne, J.; Reardon, H.; Trinh, V.; Li, E.; Farinas, J. Comparison of on-chip and off-chip microfluidic kinase assay formats. *Assay Drug Dev. Technol.* **2004**, *2* (2), 121–129. (c) Bernasconi, P.; Chen, M.; Galasinski, S.; Popa-Burke, I.; Bobasheva, A.; Coudurier, L.; Birkos, S.; Hallam, R.; Janzen, W. P. A chemogenomic analysis of the human proteome: application to enzyme families. *J. Biomol. Screening* **2007**, *12* (7), 972–982.